JCI The Journal of Clinical Investigation

SIV-specific CD8$^+$ T cells are clonotypically distinct across lymphoid and mucosal tissues

Carly E. Starke, … , David A. Price, Jason M. Brenchley

J Clin Invest. 2020;130(2):789-798. https://doi.org/10.1172/JCI129161.

Research Article AIDS/HIV Immunology

CD8$^+$ T cell responses are necessary for immune control of simian immunodeficiency virus (SIV). However, the key parameters that dictate antiviral potency remain elusive, conceivably because most studies to date have been restricted to analyses of circulating CD8$^+$ T cells. We conducted a detailed clonotypic, functional, and phenotypic survey of SIV-specific CD8$^+$ T cells across multiple anatomical sites in chronically infected rhesus macaques with high (>10,000 copies/mL plasma) or low burdens of viral RNA (<10,000 copies/mL plasma). No significant differences in response magnitude were identified across anatomical compartments. Rhesus macaques with low viral loads (VLs) harbored higher frequencies of polyfunctional CXCR5$^+$ SIV-specific CD8$^+$ T cells in various lymphoid tissues and higher proportions of unique Gag-specific CD8$^+$ T cell clonotypes in the mesenteric lymph nodes relative to rhesus macaques with high VLs. In addition, public Gag-specific CD8$^+$ T cell clonotypes were more commonly shared across distinct anatomical sites than the corresponding private clonotypes, which tended to form tissue-specific repertoires, especially in the peripheral blood and the gastrointestinal tract. Collectively, these data suggest that functionality and tissue localization are important determinants of CD8$^+$ T cell–mediated efficacy against SIV.

SIV-specific CD8+ T cells are clonotypically distinct across lymphoid and mucosal tissues

Carly E. Starke,[1] Carol L. Vinton,[1] Kristin Ladell,[2] James E. McLaren,[2] Alexandra M. Ortiz,[1] Joseph C. Mudd,[1] Jacob K. Flynn,[1] Stephen H. Lai,[1] Fan Wu,[3] Vanessa M. Hirsch,[3] Samuel Darko,[4] Daniel C. Douek,[4] David A. Price,[2,4,5] and Jason M. Brenchley[1]

[1]Barrier Immunity Section, Laboratory of Viral Diseases, National Institute of Allergy and Infectious Diseases, NIH, Bethesda, Maryland, USA. [2]Division of Infection and Immunity, Cardiff University School of Medicine, Heath Park, Cardiff, United Kingdom. [3]Nonhuman Primate Virology Section, Laboratory of Molecular Microbiology, and [4]Human Immunology Section, Vaccine Research Center, National Institute of Allergy and Infectious Diseases, NIH, Bethesda, Maryland, USA. [5]Systems Immunity Research Institute, Cardiff University School of Medicine, Heath Park, Cardiff, United Kingdom.

CD8+ T cell responses are necessary for immune control of simian immunodeficiency virus (SIV). However, the key parameters that dictate antiviral potency remain elusive, conceivably because most studies to date have been restricted to analyses of circulating CD8+ T cells. We conducted a detailed clonotypic, functional, and phenotypic survey of SIV-specific CD8+ T cells across multiple anatomical sites in chronically infected rhesus macaques with high (>10,000 copies/mL plasma) or low burdens of viral RNA (<10,000 copies/mL plasma). No significant differences in response magnitude were identified across anatomical compartments. Rhesus macaques with low viral loads (VLs) harbored higher frequencies of polyfunctional CXCR5+ SIV-specific CD8+ T cells in various lymphoid tissues and higher proportions of unique Gag-specific CD8+ T cell clonotypes in the mesenteric lymph nodes relative to rhesus macaques with high VLs. In addition, public Gag-specific CD8+ T cell clonotypes were more commonly shared across distinct anatomical sites than the corresponding private clonotypes, which tended to form tissue-specific repertoires, especially in the peripheral blood and the gastrointestinal tract. Collectively, these data suggest that functionality and tissue localization are important determinants of CD8+ T cell–mediated efficacy against SIV.

Introduction

CD8+ T cells are required to control human immunodeficiency virus (HIV) and simian immunodeficiency virus (SIV) but largely fail to protect infected humans and monkeys from eventual progression to AIDS (1). These lentiviruses replicate primarily in lymphoid tissues and preferentially infect CD4+ follicular helper T (T_{FH}) cells (2). Elite control of HIV/SIV replication has been attributed to various qualitative properties of virus-specific CD8+ T cells (3–8), including the expression of CXCR5, which allows follicular access and direct proximity to infected CD4+ T_{FH} cells (2, 9, 10). However, most studies to date have been limited to evaluations of peripheral blood samples, which may not fully recapitulate the whole-body response to HIV/SIV.

Antigen-specific CD8+ T cell populations generally incorporate several clonotypes, defined by the expression of distinct T cell receptors (TCRs) (11, 12). The composite properties of these constituent clonotypes in turn dictate the overall functionality of a given antigen-specific CD8+ T cell population (13). In the context of HIV/SIV, morphologically constrained repertoires directed against biologically variable epitopes have been associated with reproducible patterns of viral escape (14), whereas certain aspects of morphologically diverse repertoires directed against biologically constrained epitopes have been associated with protection, including the early mobilization of public clonotypes (15), which are commonly generated via convergent recombination and therefore occur in multiple individuals (16, 17), and the subsequent mobilization of cross-reactive private clonotypes (18). It nonetheless remains unclear how SIV-specific CD8+ T cells traffick in vivo to mediate these effects at sites of viral replication.

Recent work has identified discrete subsets of tissue-resident memory T cells, which occupy various epithelial, lymphoid, and mucosal sites (19–22) and differ from circulating memory T cells (23), constitutively expressing the C-type lectin CD69 and lacking the lymph node (LN) homing markers CCR7 and CD62L (24). In line with this concept of localized adaptive immunity, previous studies have revealed a degree of clonotypic disparity between circulating and mucosal SIV-specific CD8+ T cells, both in the context of acute infection (25) and in response to vaccination (26). Similarly, tissue-resident CD8+ T cells isolated from the LNs of elite controllers in another study exhibited skewed clonotypic profiles relative to specificity-matched CD8+ T cells isolated from venous blood samples, whereas the corresponding CD69− HIV-specific CD8+ T cells were clonotypically similar across the same anatomical compartments (27). These data suggest that distinct clonotypes may occupy distinct tissue niches, but to date, a comprehensive survey has not been performed across multiple anatomical sites.

In this study, we compared the clonotypic, functional, and phenotypic characteristics of SIV-specific CD8+ T cells across matched samples of peripheral blood and various lymphoid and mucosal tissues isolated from chronically infected rhesus macaques with high (>10,000 RNA copies/mL plasma) or low viral loads (VLs) (<10,000 RNA copies/mL plasma). We found

Conflict of interest: The authors have declared that no conflict of interest exists.

Submitted: March 28, 2019; **Accepted:** October 22, 2019; **Published:** January 6, 2020.
Reference information: *J Clin Invest*. 2020;130(2):789–798.
https://doi.org/10.1172/JCI129161.

Table 1. Characteristics of rhesus macaques used in this study

Animal	MHC genotype	Virus	Disease state	CD4 count[A]	Viral load[B]	Virologic status
Rh594	Mamu-A*01	smE543	Chronic	292	8,600	Low VL
Rh760	Mamu-A*01	smE543	Chronic	296	5,000	Low VL
Rh863	Mamu-A*01	smE660	Chronic	1,245	370	Low VL
Rh867	Mamu-A*01	smE660	Chronic	634	15	Low VL
Rh871	Mamu-A*01	smE660	Chronic	513	15	Low VL
RhF98	Mamu-A*01, Mamu-A*02	mac239	Chronic	560	15	Low VL
Rh591	Mamu-A*01	smE543	Chronic	186	251,000	High VL
Rh764	Mamu-A*01	smE543	Chronic	134	222,000	High VL
Rh766	Mamu-A*01	smE543	Chronic	927	50,000	High VL
Rh828	Mamu-A*01	smE543	Chronic	264	330,000	High VL
RhCL4C	Mamu-A*01	mac239	AIDS	47	470,000	High VL
RhCL86	Mamu-A*01	mac239	AIDS	91	900,000	High VL
RhDB07	Mamu-A*02	mac239	Chronic	317	550,000	High VL
RhDB17	Mamu-A*02, Mamu-B*08	mac239	AIDS	122	92,000	High VL
RhDB92	Mamu-A*02	mac239	Chronic	256	100,000	High VL
RhDCBC	Mamu-A*02	mac239	AIDS	14	1,200,000	High VL
RhDCJWA	Mamu-A*02, Mamu-B*17	mac239	AIDS	509	810,000	High VL
RhDCKJ	Mamu-A*02	mac239	AIDS	192	950,000	High VL
RhDE1A	Mamu-A*02	mac239	AIDS	246	870,000	High VL
RhDE20	Mamu-A*02	mac239	AIDS	471	67,000	High VL
RhDE2W	Mamu-A*02	mac239	AIDS	93	2,700,000	High VL
RhZA525	Mamu-A*02, Mamu-B*17	mac239	AIDS	133	1,300,000	High VL

[A]Number of $CD4^+$ T cells/μL blood. [B]Copies viral RNA/mL plasma.

that public clonotypes were commonly shared across anatomical sites, whereas private clonotypes were more often tissue specific. In addition, we identified correlates of immune control, including the presence of polyfunctional $CXCR5^+$ SIV-specific $CD8^+$ T cells in lymphoid tissues, such as the spleen and various LNs.

Results

SIV-specific $CD8^+$ T cells occur at similar frequencies in lymphoid and mucosal tissues. In preliminary experiments, we used fluorochrome-labeled pentameric complexes of Mamu-A*01-CTPYDINQM $Gag_{181–189}$ (CM9) and/or Mamu-A*02-YTSGPGIRY $Nef_{159–167}$ (Nef) and Mamu-A*02-GSENLKSLY $Gag_{71–79}$ (Gag) to evaluate the distribution of SIV-specific $CD8^+$ T cells across matched samples of peripheral blood and various tissue homogenates obtained from chronically infected rhesus macaques with high (>10,000 RNA copies/mL plasma; $n = 16$) or low VLs (<10,000 RNA copies/mL plasma; $n = 6$) (Table 1 and Supplemental Figure 1; supplemental material available online with this article; https://doi.org/10.1172/JCI129161DS1). No significant anatomical differences in response magnitude were detected between or within these outcome-defined groups (Figure 1A). Accordingly, the frequency of SIV-specific $CD8^+$ T cells in the spleen correlated with the frequencies of SIV-specific $CD8^+$ T cells in the GI tract (Figure 1B), the peripheral blood, and the axillary/inguinal lymph nodes (ALNs/ILNs) (Table 2). In contrast, the frequency of SIV-specific $CD8^+$ T cells in the peripheral blood correlated only with the frequency of SIV-specific $CD8^+$ T cells in the spleen, and the frequency of SIV-specific $CD8^+$ T cells in the mesenteric lymph nodes (MLNs) correlated only with the frequency of SIV-specific $CD8^+$ T cells in the GI tract (Table 2).

In further analyses, we compared the phenotypes of lymphoid and mucosal SIV-specific $CD8^+$ T cells, focusing on expression of the costimulatory molecules CD27 and CD28 and the tissue residency marker CD69. Strong correlations were detected between SIV-specific $CD8^+$ T cells in the spleen and SIV-specific $CD8^+$ T cells in the GI tract with respect to the expression frequencies of CD27 (Figure 1C) and CD28 (Figure 1D). No such association was observed for CD69 (Figure 1E). It was also noted that CD27, CD28, and CD69 were not differentially expressed on the surface of SIV-specific $CD8^+$ T cells as a function of VL (data not shown).

Expression of CXCR5 on SIV-specific $CD8^+$ T cells correlates inversely with VL. As expected, higher frequencies of $CD4^+$ T cells in the GI tract and higher numbers of $CD4^+$ T cells in the peripheral blood were detected in rhesus macaques with low VLs relative to rhesus macaques with high VLs (Figure 2, A and B). Moreover, the frequency of SIV-specific $CD8^+$ T cells in the GI tract correlated with the frequency of $CD4^+$ T cells in the GI tract and the number of $CD4^+$ T cells in the peripheral blood (Figure 2, C and D).

Earlier work suggested that SIV-specific $CD8^+$ T cells can enter lymphoid follicles in Asian macaques with low VLs (9, 10). In line with this observation, we found higher frequencies of $CXCR5^+$ SIV-specific $CD8^+$ T cells in the spleens of rhesus macaques with low VLs relative to rhesus macaques with high VLs (Figure 2E). To assess the biological relevance of this association, we measured SIV *gag* DNA in flow-sorted $CD4^+$ T_{FH} cells from the same tissues (Supplemental Figure 2). The frequency of $CXCR5^+$ SIV-specific $CD8^+$ T cells in the spleen correlated inversely with the amount of $CD4^+$ T_{FH} cell–associated viral DNA (Figure 2F) and the plasma burden of viral RNA (Figure 2G).

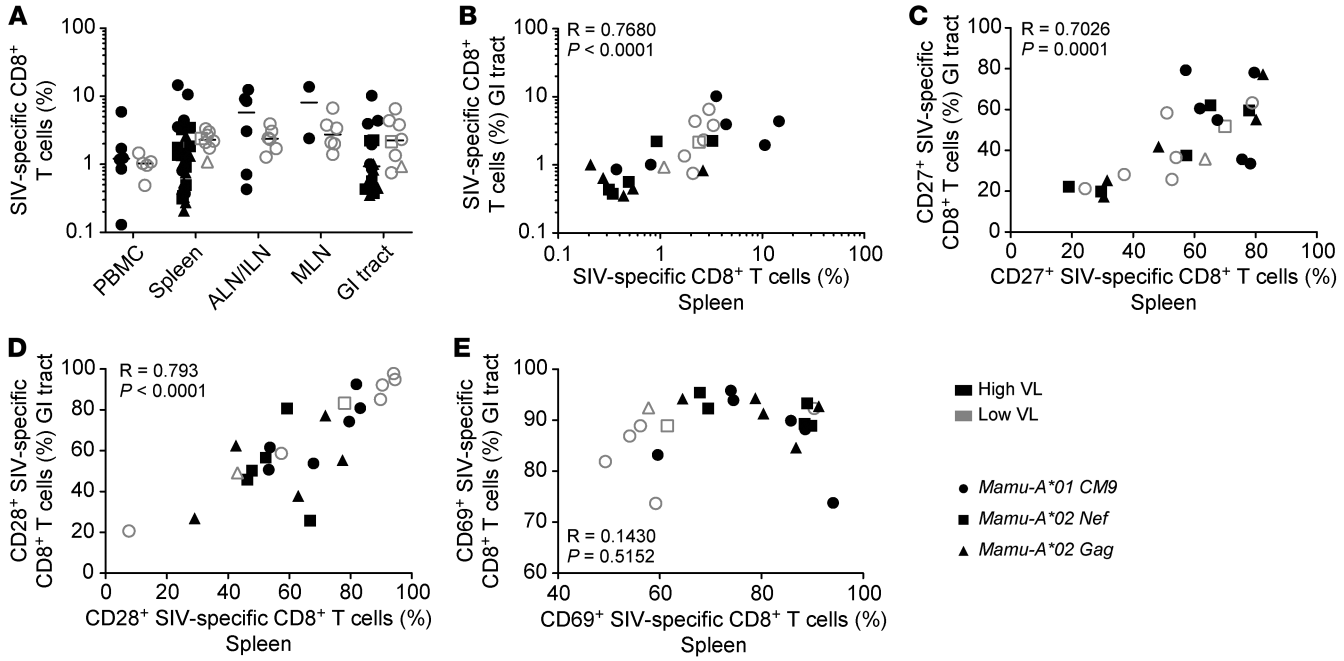

Figure 1. SIV-specific CD8⁺ T cells occur at similar frequencies in lymphoid and mucosal tissues. (**A**) Frequency of SIV-specific (CM9/Nef/Gag) CD8⁺ T cells across various anatomical sites. Horizontal bars indicate median values. GI, gastrointestinal. (**B**) Correlation between the frequency of SIV-specific CD8⁺ T cells in the GI tract and the frequency of SIV-specific CD8⁺ T cells in the spleen. (**C**–**E**) Frequency correlations for CD27⁺ (**C**), CD28⁺ (**D**), and CD69⁺ SIV-specific CD8⁺ T cells (**E**) in the GI tract versus the spleen. Data were acquired from *Mamu-A*01*⁺ and *Mamu-A*02*⁺ rhesus macaques (n = 22). Significance was determined using the Wilcoxon rank sum test (**A**) or Spearman's rank correlation with linear regression (**B**–**E**).

SIV-specific CD8⁺ T cells are polyfunctional in rhesus macaques with low VLs. To extend these findings, we assessed the functionality of SIV-specific CD8⁺ T cells in response to cognate peptide stimulation, measuring surface mobilization of CD107a and the simultaneous induction of IFN-γ, IL-2, IL-21, and TNF-α. The inclusion of IL-21 in the readout was designed to identify T_{FH}-like activity (28). Overall, SIV-specific CD8⁺ T cells were more polyfunctional in the ALNs/ILNs of rhesus macaques with low VLs relative to rhesus macaques with high VLs, but very few of these cells in either group produced IL-21 (Figure 3A).

In similar experiments, we compared the functionality of CXCR5⁺ and CXCR5⁻ SIV-specific CD8⁺ T cells, measuring surface mobilization of CD107a and intracellular granzyme B, IFN-γ, macrophage inflammatory protein–1β (MIP-1β), RANTES, and TNF-α. CXCR5⁺ SIV-specific CD8⁺ T cells were more polyfunctional in the spleens of rhesus macaques with low VLs relative to rhesus macaques with high VLs and produced a wider range of effector molecules relative to CXCR5⁻ SIV-specific CD8⁺ T cells (Figure 3B and Table 3).

SIV-specific CD8⁺ T cell clonotypes targeting CM9 are structurally diverse. The early mobilization of public clonotypes and the subsequent mobilization of cross-reactive private clonotypes directed against biologically constrained epitopes have been associated with enhanced control of HIV/SIV (15, 18). We therefore used an unbiased molecular approach to characterize all expressed TCRβ locus (*TRB*) gene rearrangements in flow-sorted Mamu-A*01–restricted CM9-specific CD8⁺ T cell populations (Supplemental Figure 2) isolated at necropsy from each anatomical site in rhesus macaques with high (Supplemental Figure 3) or low VLs (Supplemental Figure 4). Data were normalized before analysis to correct for differences in sample size (29, 30). The number of unique clonotypes per anatomical site was similar in rhesus macaques with high (median 6, range 1–16) and low VLs (median 7, range 1–13). Moreover, no consistent anatomical differences in repertoire diversity were apparent between or within these outcome-defined groups, and accordingly, no correlations were detected between repertoire diversity and either the amount of CD4⁺ T_{FH} cell–associated viral DNA or the plasma burden of viral RNA (data not shown and Figure 4A). There were some conspicuous anatomical differences in repertoire similarity, however, most notably between lymphoid and mucosal sites in certain rhesus macaques with high or low VLs (Figure 4B).

Table 2. Frequency correlations for SIV-specific CD8⁺ T cells across various anatomical sites

	Spleen	ALN/ILN	MLN	GI tract
PBMC	0.6364, 0.0402	0.3736, 0.2562	0.4643, 0.3024	0.4273, 0.1928
Spleen		0.8196, 0.0017	0.6905, 0.0694	0.7680, <0.0001
ALN/ILN			0.6467, 0.0911	0.6830, 0.0171
MLN				0.9048, 0.0046

Data were acquired from *Mamu-A*01*⁺ and *Mamu-A*02*⁺ rhesus macaques (n = 22). Significance was determined using Spearman's rank correlation with linear regression. Each cell shows the corresponding R (left) and P value (right). Details as in Figure 1B.

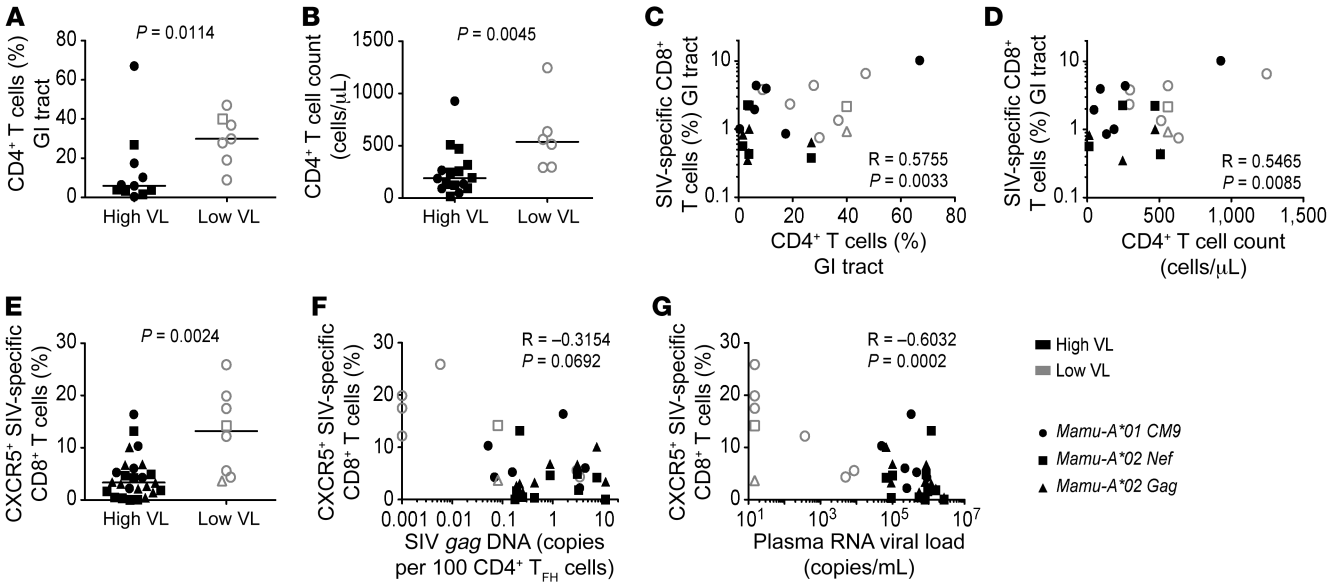

Figure 2. Expression of CXCR5 on SIV-specific CD8⁺ T cells correlates inversely with VL. (**A**) Frequency of CD4⁺ T cells in the GI tract. (**B**) Number of CD4⁺ T cells in the peripheral blood. (**C**) Correlation between the frequency of SIV-specific CD8⁺ T cells in the GI tract and the frequency of CD4⁺ T cells in the GI tract. (**D**) Correlation between the frequency of SIV-specific CD8⁺ T cells in the GI tract and the number of CD4⁺ T cells in the peripheral blood. (**E**) Frequency of CXCR5⁺ SIV-specific CD8⁺ T cells in the spleen. (**F**) Correlation between the frequency of CXCR5⁺ SIV-specific CD8⁺ T cells in the spleen and the amount of viral DNA in CD4⁺ T_{FH} cells. (**G**) Correlation between the frequency of CXCR5⁺ SIV-specific CD8⁺ T cells in the spleen and VL. Data were acquired from *Mamu-A*01*⁺ and *Mamu-A*02*⁺ rhesus macaques (n = 22). Horizontal bars indicate median values (**A**, **B**, and **E**). Significance was determined using the Mann-Whitney U test (**A**, **B**, and **E**) or Spearman's rank correlation with linear regression (**C**, **D**, **F**, and **G**).

A vast majority of CM9-specific clonotypes in both groups incorporated CDR3β loops spanning 14 amino acids, with equivalent representation at each anatomical site (Supplemental Figure 5). Irrespective of anatomical location, preferential use of *TRBV6-1* and *TRBV9* was observed in rhesus macaques with high VLs (Figure 4C), and preferential use of *TRBV6-1*, *TRBV10-2*, and *TRBV13* was observed in rhesus macaques with low VLs (Figure 4D). Similarly, preferential use of *TRBJ1-5* and *TRBJ2-1* was observed in rhesus macaques with high VLs (Supplemental Figure 6A), and preferential use of *TRBJ1-5* was observed in rhesus macaques with low VLs (Supplemental Figure 6B). No clear motifs were observed among non–germline-encoded CDR3β residues, irrespective of VL (Figure 4, E and F).

SIV-specific CD8⁺ T cell clonotypes targeting CM9 are anatomically discrete. To substantiate the observed anatomical differences in repertoire similarity, we assessed the distribution of CM9-specific clonotypes across peripheral blood and tissue sites, again comparing rhesus macaques with high versus low VLs. A degree of clonotype sharing was apparent in each individual rhesus macaque, most notably between the spleen and the peripheral blood and between the MLNs and the GI tract (Figure 5, A and B). However, many clonotypes were either unique to a particular anatomical site or preferentially located in a particular anatomical site, most commonly the GI tract (Figure 5, A and B). No obvious anatomical differences in clonotype sharing were detected between groups, although unique clonotypes were significantly more common in the MLNs of rhesus macaques with low VLs relative to rhesus macaques with high VLs (Figure 5C). Equivalent levels of sharing between groups were also observed for clonotypes stratified by the number of occupied sites (Figure 5D). In general, the number of anatomical sites occupied by a given clonotype increased as the frequency of a given clonotype increased at any given anatomical site, and this was true across all sampled tissues (Figure 5E and Table 4). However, there were exceptions to this pattern, especially in the GI tract, where some clonotypes occurred at high frequencies with no sharing (e.g., rhesus macaque 591) or sharing restricted to the MLNs (e.g., rhesus macaque 863), and other clonotypes occurred at low frequencies with sharing across all anatomical sites (e.g., rhesus macaques 760 and F98) (Figure 5, A and B). Moreover, approximately 40% of clonotypes were unique to each site, rising to more than 55% in the peripheral blood and the GI tract, and most of the shared clonotypes in the peripheral blood were found in the spleen but not in the GI tract (Figure 5F). These clonotypically distinct SIV-specific CD8⁺ T cell populations were nonetheless functionally equivalent across various tissue sites, at least after stimulation with nonlimiting concentrations of CM9 (Figure 5G).

Public clonotypes were identified on the basis of sharing at the amino acid level across more than 1 rhesus macaque in our cohort and/or across previously reported data sets from other rhesus macaques (refs. 14, 15, 31 and Figure 6, A and B). No significant differences in the anatomical distribution of public clonotypes were detected between or within groups (Figure 6C). However, public clonotypes with identical nucleotide sequences were shared across anatomical sites more commonly than private clonotypes in individual rhesus macaques, irrespective of VL (Figure 6D).

Discussion

Virus-specific CD8⁺ T cells are necessary for the control of HIV and SIV (32–34). However, the precise determinants of immune

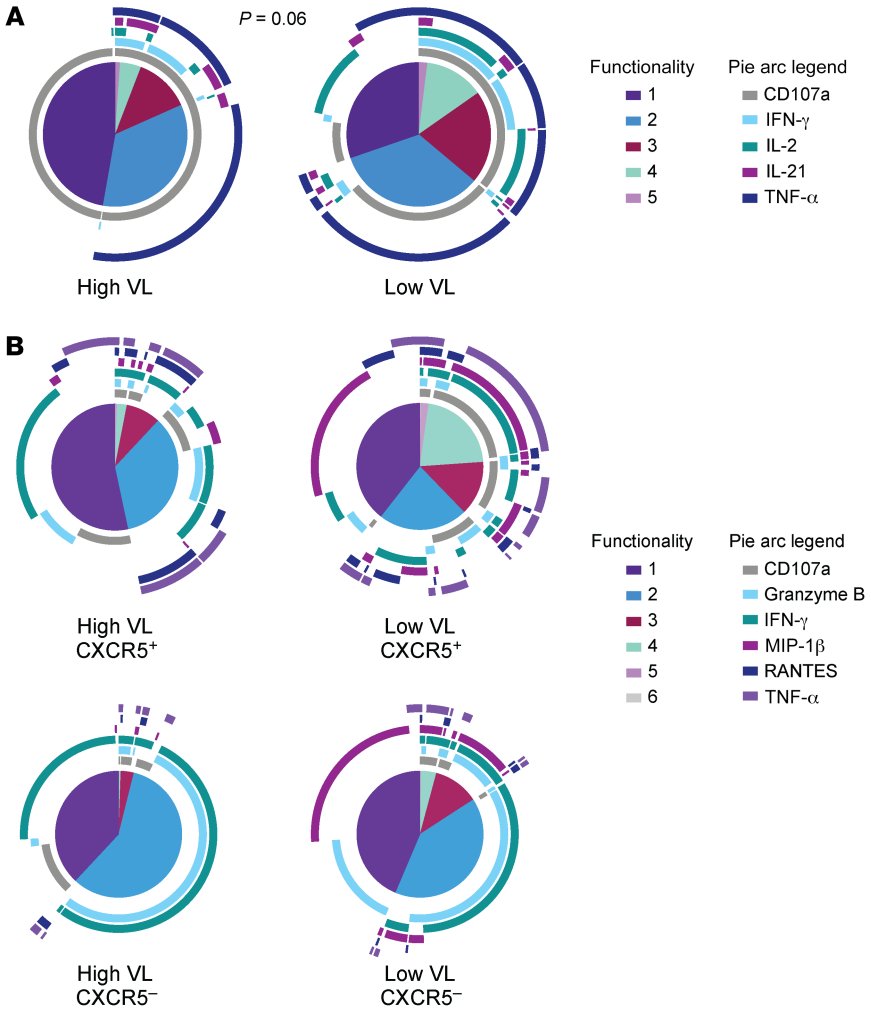

Figure 3. SIV-specific CD8⁺ T cells are polyfunctional in rhesus macaques with low VLs. (**A**) Pie charts depict relative expression of CD107a, IFN-γ, IL-2, IL-21, and/or TNF-α among memory CD8⁺ T cells in response to stimulation of ALNs/ILNs with overlapping peptides spanning SIV Gag (n = 6 *Mamu-A*01*⁺ rhesus macaques per group). (**B**) Pie charts depict relative expression of CD107a, granzyme B, IFN-γ, MIP-1β, RANTES, and/or TNF-α among CXCR5⁺ or CXCR5⁻ memory CD8⁺ T cells in response to stimulation of splenocytes with overlapping peptides spanning SIV Gag (n = 4 *Mamu-A*01*⁺ rhesus macaques per group). Significance was determined using the permutation test in Simplified Presentation of Incredibly Complex Evaluations (SPICE) (detailed in Table 3).

efficacy remain unclear, potentially because current paradigms are based primarily on studies of circulating CD8⁺ T cells. We report here that SIV-specific CD8⁺ T cells are clonotypically distinct across multiple anatomical compartments in rhesus macaques with chronic infection or AIDS. Public clonotypes were commonly shared across anatomical sites in individual rhesus macaques, as were the more dominant clonotypes at any particular anatomical site, but overall, approximately 40% of clonotypes were site specific, and unique clonotypes were observed most often in the peripheral blood and the GI tract. Moreover, rhesus macaques with low VLs harbored higher frequencies of polyfunctional CXCR5⁺ SIV-specific CD8⁺ T cells in various lymphoid tissues, such as the spleen and the ALNs/ILNs.

Expression of CXCR5 is required for entry into B cell follicles (35, 36). We found that the frequency of CXCR5⁺ SIV-specific CD8⁺ T cells in the spleen correlated inversely with viral replication, measured in terms of CD4⁺ T_{FH} cell–associated viral DNA and plasma viral RNA. Although these findings are consistent with the hypothesis that follicular access licenses the optimal delivery of antiviral effector functions (37–39), it is important to note that high levels of antigen expression can exhaust follicular CXCR5⁺ virus-specific CD8⁺ T cells as a consequence of sustained activation via the TCR (40). This phenomenon may explain, at least in part, the preferential occurrence of CXCR5⁺ SIV-specific CD8⁺ T cells in rhesus macaques with low VLs. Follicular CXCR5⁺ SIV-specific CD8⁺ T cells are nonetheless optimally positioned to suppress viral replication in vivo, potentially via noncytolytic mechanisms (41).

Our current understanding of HIV/SIV-specific CD8⁺ T cell responses is derived mainly from studies of peripheral blood, which is easily accessible in humans and other primates (1, 3, 4, 14, 15, 18, 32–34, 42). Other windows may provide better insights, however, because these viruses replicate in lymphoid tissues, and very few lymphocytes in the total body pool circulate at any

Table 3. Functionality comparisons for CXCR5⁺ versus CXCR5⁻ memory CD8⁺ T cells in rhesus macaques with high versus low VLs

	Low VL CXCR5⁺	High VL CXCR5⁻	Low VL CXCR5⁻
High VL CXCR5⁺	0.0124	0.1132	0.0206
Low VL CXCR5⁺		0.0278	0.2641
High VL CXCR5⁻			0.0583

Data were acquired from *Mamu-A*01*⁺ rhesus macaques (n = 4). Significance was determined using the permutation test in SPICE. Each cell shows the corresponding P value. Details as in Figure 3B.

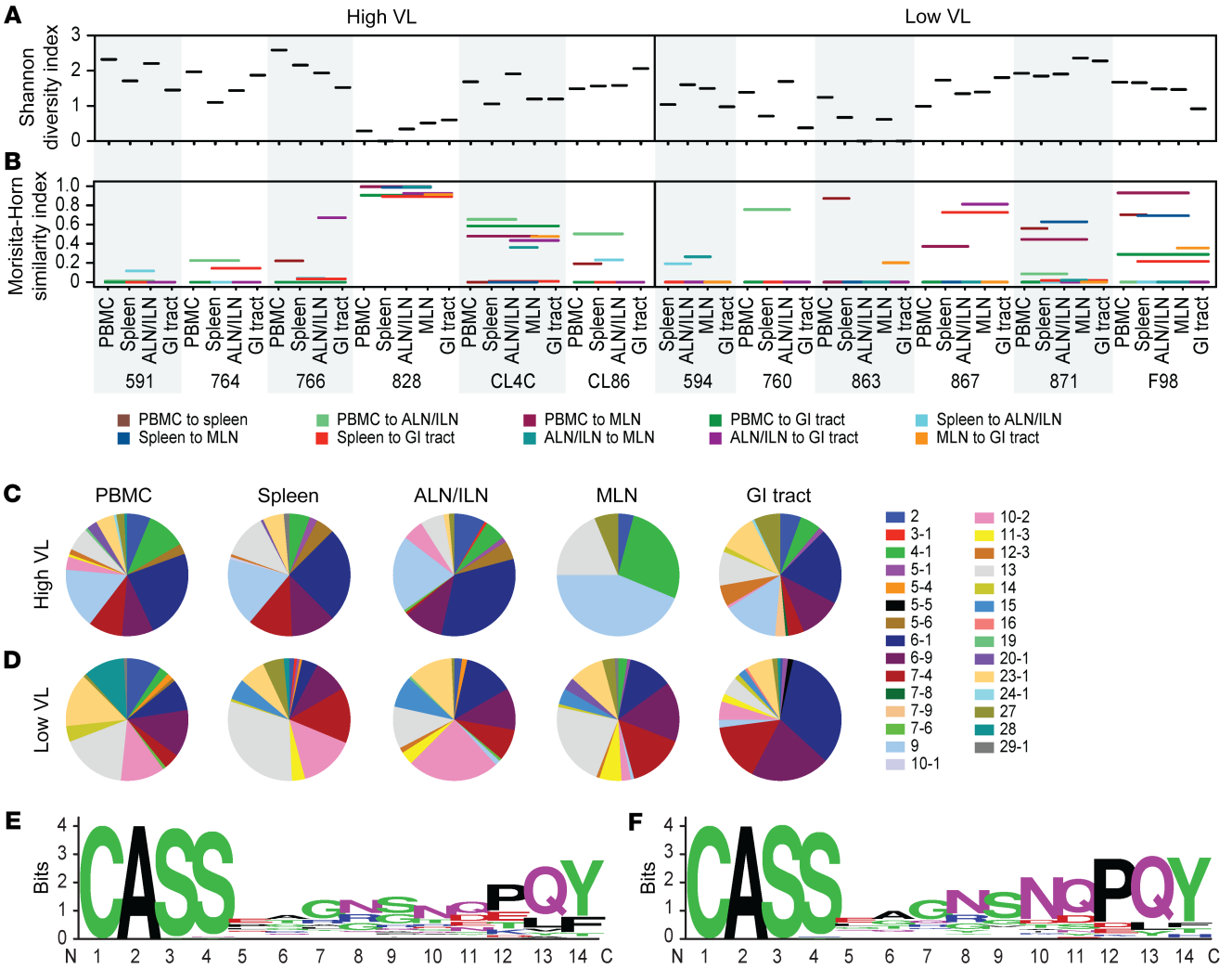

Figure 4. Clonotypic architecture of CM9-specific CD8⁺ T cell populations. (**A**) Repertoire diversity in rhesus macaques with high (n = 6) or low VLs (n = 6). (**B**) Repertoire similarity in rhesus macaques with high (n = 6) or low VLs (n = 6). (**C**) *TRBV* gene use in rhesus macaques with high VLs (n = 6). (**D**) *TRBV* gene use in rhesus macaques with low VLs (n = 6). (**E**) CDR3β amino acid use in rhesus macaques with high VLs (n = 6). (**F**) CDR3β amino acid use in rhesus macaques with low VLs (n = 6). Significance was determined using the permutation test in SPICE (**C** and **D**).

given time (43). In line with previous studies, we found a degree of clonotype sharing across anatomical compartments (25, 26, 44), which has likewise been reported in the context of influenza virus infection (45). However, we also identified anatomically unique clonotypes, most frequently in the peripheral blood and the GI tract. The clonotypic disparity between peripheral blood and lymphoid tissues is consistent with the recent description of tissue-resident HIV-specific CD8⁺ T cells (27), which provide durable antiviral immunity at the site(s) of viral challenge/replication (27, 46, 47). Our data therefore suggest 2 mutually inclusive possibilities. The first is that individual CD8⁺ T cells are primed in situ and do not traffick extensively between anatomical compartments during chronic infection, implying that systemic vaccination may be required to elicit long-term immunity against HIV/SIV (26). The second is that public clonotypes are more readily primed during the early stages of infection as a function of prevalence within the naive pool, which can be attributed to convergent recombination (48, 49), and subsequently form highly stable tissue-resident populations, which are then more likely to be shared across sites of viral replication (27, 50). Longitudinal studies will be necessary to address these possibilities and determine which route(s) of vaccine delivery are likely to favor the generation of effective immunity against HIV/SIV.

In summary, we have demonstrated that SIV-specific CD8⁺ T cells are clonotypically, functionally, and phenotypically distinct across multiple anatomical sites in outcome-defined groups of rhesus macaques with chronic infection or AIDS. A greater understanding of these anatomical complexities may therefore be required to identify the key attributes of effective virus-specific CD8⁺ T cell responses, which in turn may inform the rational design of next-generation vaccines against HIV/SIV.

Methods

Study design. The goal of this study was to assess the functional and phenotypic characteristics of SIV-specific CD8⁺ T cell clonotypes across distinct anatomical compartments in rhesus macaques (*Macaca*

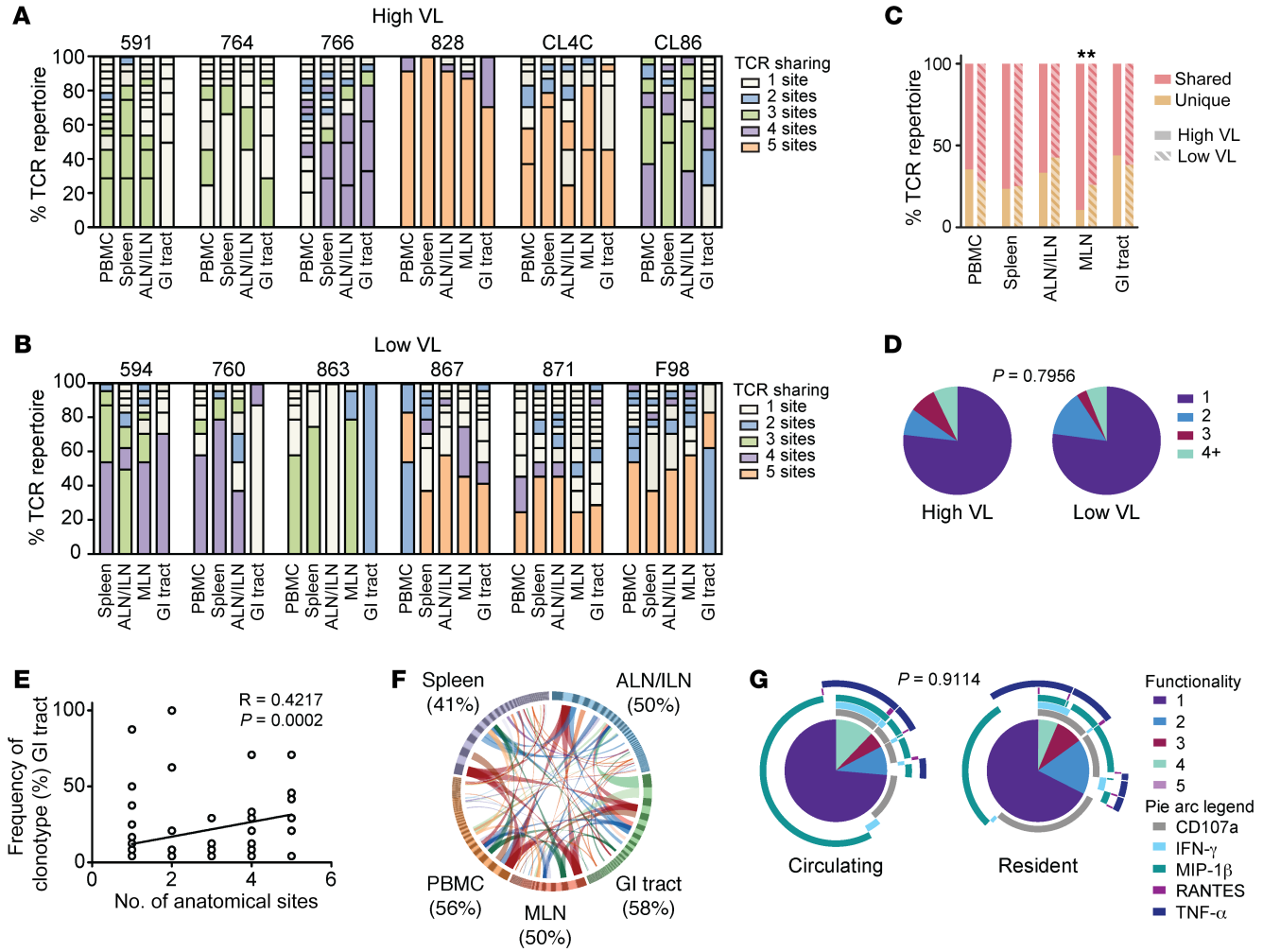

Figure 5. CM9-specific CD8⁺ T cell clonotypes are anatomically discrete. (**A**) Frequency of individual clonotypes across various anatomical sites in rhesus macaques with high VLs. (**B**) Frequency of individual clonotypes across various anatomical sites in rhesus macaques with low VLs. (**C**) Proportion of clonotypes detected in 1 (unique) or more than 1 (shared) anatomical site in rhesus macaques with high (n = 6) or low VLs (n = 6). Significance was determined using the χ^2 test. $^{**}P < 0.01$. (**D**) Proportion of clonotypes shared across the indicated number of anatomical sites in rhesus macaques with high (n = 6) or low VLs (n = 6). Significance was determined using the Mann-Whitney U test. (**E**) Correlation between the number of occupied anatomical sites and clonotype frequency in the GI tract. Significance was determined using Spearman's rank correlation with linear regression. (**F**) Schematic representation of clonotype sharing across distinct anatomical sites (n = 12 *Mamu-A*01*⁺ rhesus macaques). Values in parentheses refer to unique clonotypes at each anatomical site (%). (**G**) Pie charts depict relative expression of CD107a, IFN-γ, MIP-1β, RANTES, and/or TNF-α among clonotypically distinct (TCR Vβ1⁺ or TCR Vβ23⁺) CM9-specific memory CD8⁺ T cells in response to stimulation of various tissue homogenates with overlapping peptides spanning SIV Gag (n = 4 *Mamu-A*01*⁺ rhesus macaques per group). Clonotypes found in multiple tissues (circulating) were distinguished from clonotypes found in 1 tissue (resident). Significance was determined using the permutation test in SPICE.

mulatta) with high (>10,000 RNA copies/mL plasma; n = 16) or low VLs (<10,000 RNA copies/mL plasma; n = 6) during the chronic phase of infection with SIVmac239, SIVsmE543, or SIVsmE660 (Table 1 and Supplemental Figure 1). Selection criteria included the availability of cryopreserved tissue homogenates. PBMCs, spleen, ALNs, ILNs, MLNs, colon, and jejunum were obtained at necropsy from *Mamu-A*01*⁺ (n = 12) and *Mamu-A*02*⁺ rhesus macaques (n = 11) with established SIV infection or AIDS (Table 1). Samples were homogenized as described previously (51). Clinical endpoints were defined as (a) weight loss more than 25%; (b) major organ failure or medical conditions unresponsive to treatment; (c) complete anorexia for 4 days; (d) inability to consume sufficient nutrients to maintain body weight without assistance for 7 days; (e) distress vocalization unresponsive to intervention for 7 days; and/or (f) tumors arising from other than experimental means that impaired movement, ulcerated, or grew to more than 10% of body weight. Euthanasia was performed according to guidelines established by the American Veterinary Medical Association.

Flow cytometric sorting of SIV-specific CD8⁺ T cells. Tissue homogenates were washed twice in RPMI 1640 medium supplemented with 10% fetal bovine serum, 2 mM L-glutamine, and 1% penicillin/streptomycin (all from HyClone, GE Healthcare Life Sciences). SIV-specific CD8⁺ T cells were identified using CM9 and/or Nef and Gag Pro5 MHC Class I Pentamers (ProImmune). Surface markers were identified using pretitrated concentrations of the following antibodies: (a) anti-CD8a (RPA-T8) and anti-CXCR5 (MU5UBEE) from eBioscience; (b) anti-CD3 (SP34-2), anti-CD8a (SK1), anti-CD27 (O323), anti-CD69 (FN50), and anti-CCR7 (3D12) from BD Biosciences; (c) anti-CD4 (OKT4), anti-CD95 (DX2), and anti–PD-1 (EH12.2H7) from

Table 4. Correlations between the number of occupied anatomical sites and clonotype frequency at each anatomical site

Tissue	*R*	*P*
PBMC	0.4470	<0.0001
Spleen	0.5621	<0.0001
ALN/ILN	0.4718	<0.0001
MLN	0.5074	0.0003
GI tract	0.4217	0.0002

Data were acquired from *Mamu-A*01*$^+$ rhesus macaques (n = 12). Significance was determined using Spearman's rank correlation with linear regression. Details as in Figure 5E.

BioLegend; and (d) anti-CD28 (CD28.2) from Beckman Coulter. Bulk CD4$^+$ T_{FH} cells and SIV-specific CD8$^+$ T cells were flow-sorted using a FACSAria (BD Biosciences). Bulk CD4$^+$ T_{FH} cells were defined as live, CD3$^+$, CD4$^+$, CD28$^+$, CD95$^+$, CXCR5$^+$, PD-1$^+$ lymphocytes, and SIV-specific CD8$^+$ T cells were defined as live, CD3$^+$, CD8$^+$, CM9/Nef/Gag$^+$ lymphocytes (Supplemental Figure 2).

Functional analysis of SIV-specific CD8$^+$ T cells. Cell suspensions were stimulated with a pool of peptides spanning SIV Gag (15-mers overlapping by 11 amino acids) at a final concentration of 2 μg/peptide/10^6 cells in the presence of anti-CD28 (CD28.2; Beckman Coulter), anti-CD107a (H4A3; BioLegend), brefeldin A (1 μg/mL; MilliporeSigma), and monensin (1 μg/mL; BD Biosciences) for 16 hours at 37°C. After stimulation, cells were washed in PBS, stained for surface markers, fixed/permeabilized, and stained for intracellular markers. The following antibodies were used in these experiments: (a) anti-CD4 (OKT4), anti-CXCR5 (MU5UBEE), and anti–IL-21 (3A3-N2) from eBioscience; (b) anti-CD3 (SP34-2), anti-CD8a (SK1), anti-CD95 (DX2), anti–granzyme B (GB11), anti–IL-2 (MQ1-17H12), anti–MIP-1β (D21-1351), and anti-RANTES (2D5) from BD Biosciences; (c) anti–IFN-γ (4S.B3) and anti–TNF-α (MAb11) from BioLegend; and (d) anti–TCR Vβ1 (BL37.2) and anti–TCR Vβ23 (AF23) from Beckman Coulter. Data were acquired using an LSR Fortessa (BD Biosciences). SIV-specific CD8$^+$ T cells were defined as live, CD3$^+$, CD8$^+$, function$^+$/pentamer$^+$ lymphocytes (Supplemental Figure 2). Functional profiles were analyzed using SPICE v5.35 (National Institute of Allergy and Infectious Diseases).

Quantification of cell-associated SIV DNA. SIV DNA was quantified in CD4$^+$ T_{FH} cells as described previously (52, 53). Briefly,

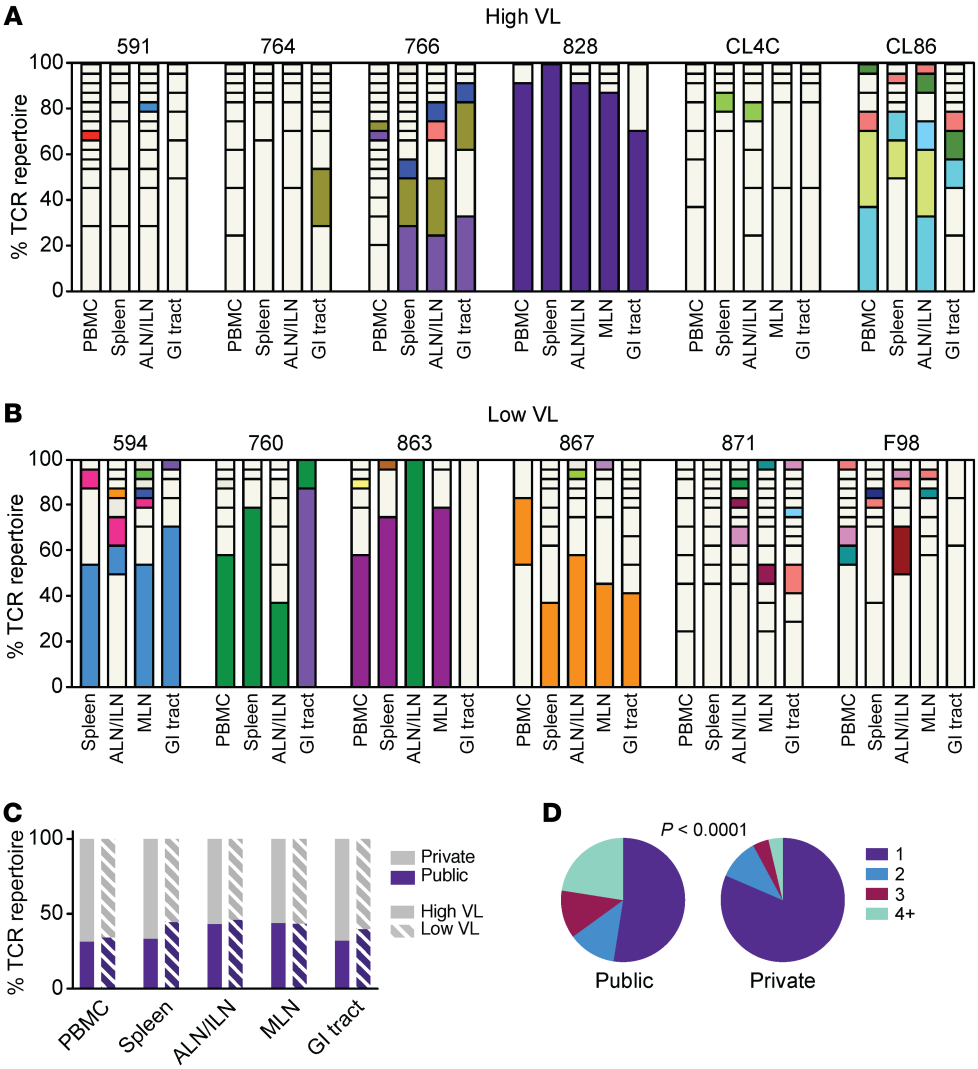

Figure 6. Public CM9-specific CD8$^+$ T cell clonotypes are commonly shared across multiple anatomical sites. (**A**) Frequency of public (colored bars) or private clonotypes (white bars) across various anatomical sites in rhesus macaques with high VLs. (**B**) Frequency of public (colored bars) or private clonotypes (white bars) across various anatomical sites in rhesus macaques with low VLs. (**C**) Proportion of public or private clonotypes detected at each anatomical site in rhesus macaques with high (n = 6) or low VLs (n = 6). Significance was determined using the χ^2 test. (**D**) Proportion of public or private clonotypes shared across the indicated number of anatomical sites in *Mamu-A*01*$^+$ rhesus macaques (n = 12). Significance was determined using the Mann-Whitney U test.

flow-sorted cells were lyzed using 25 μL of a 1:100 dilution of proteinase K (Roche) in 10 mM Tris-HCl (pH 8.4). Quantitative PCRs were performed in duplicate using 5 μL of cell lysate per reaction with TaqMan Master Mix (Thermo Fisher Scientific) over 50 cycles of 95°C for 15 seconds and 60°C for 1 minute after a single holding step of 95°C for 5 minutes. SIV_{mac239} *gag* was amplified using the forward primer GTCTGCGTCATYTGGTGCATTC and the reverse primer CACTAGYTGTCTCTGCACTATRTGTTTTG with the probe CTTCRTCAGTYTGTTTCACTTTCTCTTCTGCG. $SIV_{smE543/smE660}$ *gag* was amplified using the forward primer GGCAGGAAAATCCCTAGCAG and the reverse primer GCCCTTACTGCCTTCACTCA with the probe AGTCCCTGTTCRGGCGCCAA. Cell numbers were quantified relative to monkey albumin (54). Reactions were processed using a StepOnePlus Real-Time PCR System (Applied Biosystems, Thermo Fisher Scientific), and template copies were calculated using StepOne Software (Applied Biosystems, Thermo Fisher Scientific).

Clonotype analysis. Pentamer-labeled $CD8^+$ T cells were flow-sorted viably into 100 μL of RNAlater (MilliporeSigma). All expressed *TRB* gene rearrangements were amplified without bias using a template-switch anchored reverse transcription PCR as described previously (55). Sequences were aligned using Sequencher v5.4.6 (Gene Codes Corporation). *TRBV* and *TRBJ* genes were identified according to the ImMunoGeneTics nomenclature (56). Data were normalized using a randomization procedure to account for differences in sample size as described previously (29, 30). Repertoire diversity was assessed using the Shannon diversity index (29), and repertoire similarity was assessed using the Morisita-Horn similarity index (30). Anatomical overlap was visualized using Circos (http://circos.ca/) and InteractiVenn (http://www.interactivenn.net/), and amino acid use was visualized using WebLogo (https://weblogo.berkeley.edu/).

Statistics. Matched groups were compared using the Wilcoxon rank sum test. Unmatched groups were compared using the Mann-Whitney *U* test. Correlations were evaluated using Spearman's rank correlation with linear regression. Proportions were compared using the χ^2 test. All statistical analyses were performed using Prism v7.0 (GraphPad Software Inc.). *P* values less than 0.05 were considered significant. Functional profiles were compared using the permutation test with relative expression values in SPICE v5.35 (National Institute of Allergy and Infectious Diseases).

Study approval. Experimental procedures were approved by the National Institute of Allergy and Infectious Diseases Division of Intramural Research Animal Care and Use Program as part of the NIH Intramural Research Program (protocols LMM6 and LVD26). Rhesus macaques were housed and sustained in accordance with standards established by the Association for Assessment and Accreditation of Laboratory Animal Care.

Author contributions

CES, CLV, AMO, JCM, JKF, SHL, FW, and JMB performed experiments. CES, CLV, JCM, SD, and JMB analyzed data. KL, JEM, AMO, FW, VMH, DCD, and DAP provided critical resources. CES and JMB designed the project. CES, DAP, and JMB wrote the manuscript.

Acknowledgments

We thank Heather Kendall, JoAnne Swerczek, Richard Herbert, and all veterinary staff at the NIH Animal Center. This study was supported in part by the Division of Intramural Research, National Institute of Allergy and Infectious Diseases, NIH. DAP is a Wellcome Trust Senior Investigator (100326/Z/12/Z).

Address correspondence to: Jason M. Brenchley, 4 Memorial Drive, Room 211, 9000 Rockville Pike, Bethesda, Maryland 20892, USA. Phone: 301.496.1498; Email: jbrenchl@niaid.nih.gov.

1. McBrien JB, Kumar NA, Silvestri G. Mechanisms of $CD8^+$ T cell-mediated suppression of HIV/SIV replication. *Eur J Immunol*. 2018;48(6):898–914.
2. Fukazawa Y, et al. B cell follicle sanctuary permits persistent productive simian immunodeficiency virus infection in elite controllers. *Nat Med*. 2015;21(2):132–139.
3. Betts MR, et al. HIV nonprogressors preferentially maintain highly functional HIV-specific $CD8^+$ T cells. *Blood*. 2006;107(12):4781–4789.
4. Sáez-Cirión A, et al. HIV controllers exhibit potent CD8 T cell capacity to suppress HIV infection ex vivo and peculiar cytotoxic T lymphocyte activation phenotype. *Proc Natl Acad Sci USA*. 2007;104(16):6776–6781.
5. Sáez-Cirión A, Pancino G, Sinet M, Venet A, Lambotte O, ANRS EP36 HIV Controllers Study Group. HIV controllers: how do they tame the virus? *Trends Immunol*. 2007;28(12):532–540.
6. Deeks SG, Walker BD. Human immunodeficiency virus controllers: mechanisms of durable virus control in the absence of antiretroviral therapy. *Immunity*. 2007;27(3):406–416.
7. Feinberg MB, Ahmed R. Born this way? Understanding the immunological basis of effective HIV control. *Nat Immunol*. 2012;13(7):632–634.
8. Hersperger AR, Migueles SA, Betts MR, Connors M. Qualitative features of the HIV-specific $CD8^+$ T-cell response associated with immunologic control. *Curr Opin HIV AIDS*. 2011;6(3):169–173.
9. Mylvaganam GH, et al. Dynamics of SIV-specific $CXCR5^+$ CD8 T cells during chronic SIV infection. *Proc Natl Acad Sci USA*. 2017;114(8):1976–1981.
10. Ferrando-Martinez S, et al. Accumulation of follicular $CD8^+$ T cells in pathogenic SIV infection. *J Clin Invest*. 2018;128(5):2089–2103.
11. Li H, Ye C, Ji G, Han J. Determinants of public T cell responses. *Cell Res*. 2012;22(1):33–42.
12. Miles JJ, Douek DC, Price DA. Bias in the αβ T-cell repertoire: implications for disease pathogenesis and vaccination. *Immunol Cell Biol*. 2011;89(3):375–387.
13. Appay V, Douek DC, Price DA. $CD8^+$ T cell efficacy in vaccination and disease. *Nat Med*. 2008;14(6):623–628.
14. Price DA, et al. T cell receptor recognition motifs govern immune escape patterns in acute SIV infection. *Immunity*. 2004;21(6):793–803.
15. Price DA, et al. Public clonotype usage identifies protective Gag-specific $CD8^+$ T cell responses in SIV infection. *J Exp Med*. 2009;206(4):923–936.
16. Venturi V, et al. Sharing of T cell receptors in antigen-specific responses is driven by convergent recombination. *Proc Natl Acad Sci USA*. 2006;103(49):18691–18696.
17. Venturi V, Price DA, Douek DC, Davenport MP. The molecular basis for public T-cell responses? *Nat Rev Immunol*. 2008;8(3):231–238.
18. Ladell K, et al. A molecular basis for the control of preimmune escape variants by HIV-specific $CD8^+$ T cells. *Immunity*. 2013;38(3):425–436.
19. Gebhardt T, Wakim LM, Eidsmo L, Reading PC, Heath WR, Carbone FR. Memory T cells in nonlymphoid tissue that provide enhanced local immunity during infection with herpes simplex virus. *Nat Immunol*. 2009;10(5):524–530.
20. Masopust D, et al. Dynamic T cell migration program provides resident memory within intestinal epithelium. *J Exp Med*. 2010;207(3):553–564.
21. Masopust D, Vezys V, Marzo AL, Lefrançois L. Preferential localization of effector memory cells in nonlymphoid tissue. *Science*. 2001;291(5512):2413–2417.
22. Wakim LM, Waithman J, van Rooijen N, Heath WR, Carbone FR. Dendritic cell-induced memory T cell activation in nonlymphoid tissues. *Science*. 2008;319(5860):198–202.
23. Schenkel JM, Fraser KA, Masopust D. Cutting edge: resident memory CD8 T cells occupy frontline niches in secondary lymphoid organs. *J Immunol*. 2014;192(7):2961–2964.
24. Mackay LK, et al. The developmental pathway for $CD103^+CD8^+$ tissue-resident memory T cells of skin. *Nat Immunol*. 2013;14(12):1294–1301.

25. Sircar P, Furr KL, Dorosh LA, Letvin NL. Clonal repertoires of virus-specific CD8$^+$ T lymphocytes are shared in mucosal and systemic compartments during chronic simian immunodeficiency virus infection in rhesus monkeys. *J Immunol*. 2010;185(4):2191–2199.
26. Sircar P, Furr KL, Letvin NL. Systemic vaccination induces clonally diverse SIV-specific CD8$^+$ T-cell populations in systemic and mucosal compartments. *Mucosal Immunol*. 2013;6(1):93–103.
27. Buggert M, et al. Identification and characterization of HIV-specific resident memory CD8$^+$ T cells in human lymphoid tissue. *Sci Immunol*. 2018;3(24):eaar4526.
28. Bryant VL, et al. Cytokine-mediated regulation of human B cell differentiation into Ig-secreting cells: predominant role of IL-21 produced by CXCR5$^+$ T follicular helper cells. *J Immunol*. 2007;179(12):8180–8190.
29. Venturi V, Kedzierska K, Turner SJ, Doherty PC, Davenport MP. Methods for comparing the diversity of samples of the T cell receptor repertoire. *J Immunol Methods*. 2007;321(1–2):182–195.
30. Venturi V, Kedzierska K, Tanaka MM, Turner SJ, Doherty PC, Davenport MP. Method for assessing the similarity between subsets of the T cell receptor repertoire. *J Immunol Methods*. 2008;329(1–2):67–80.
31. Shugay M, et al. VDJdb: a curated database of T-cell receptor sequences with known antigen specificity. *Nucleic Acids Res*. 2018;46(D1):D419–D427.
32. Schmitz JE, et al. Control of viremia in simian immunodeficiency virus infection by CD8+ lymphocytes. *Science*. 1999;283(5403):857–860.
33. Koup RA, et al. Temporal association of cellular immune responses with the initial control of viremia in primary human immunodeficiency virus type 1 syndrome. *J Virol*. 1994;68(7):4650–4655.
34. Ogg GS, et al. Quantitation of HIV-1-specific cytotoxic T lymphocytes and plasma load of viral RNA. *Science*. 1998;279(5359):2103–2106.
35. Ansel KM, McHeyzer-Williams LJ, Ngo VN, McHeyzer-Williams MG, Cyster JG. In vivo-activated CD4 T cells upregulate CXC chemokine receptor 5 and reprogram their response to lymphoid chemokines. *J Exp Med*. 1999;190(8):1123–1134.
36. Haynes NM, Allen CD, Lesley R, Ansel KM, Killeen N, Cyster JG. Role of CXCR5 and CCR7 in follicular Th cell positioning and appearance of a programmed cell death gene-1^{high} germinal center-associated subpopulation. *J Immunol*. 2007;179(8):5099–5108.
37. Connick E, et al. Compartmentalization of simian immunodeficiency virus replication within secondary lymphoid tissues of rhesus macaques is linked to disease stage and inversely related to localization of virus-specific CTL. *J Immunol*. 2014;193(11):5613–5625.
38. He R, et al. Follicular CXCR5-expressing CD8$^+$ T cells curtail chronic viral infection. *Nature*. 2016;537(7620):412–428.
39. Li S, et al. Simian immunodeficiency virus-producing cells in follicles are partially suppressed by CD8$^+$ cells *in vivo*. *J Virol*. 2016;90(24):11168–11180.
40. Wherry EJ, Kurachi M. Molecular and cellular insights into T cell exhaustion. *Nat Rev Immunol*. 2015;15(8):486–499.
41. Reuter MA, et al. HIV-specific CD8$^+$ T cells exhibit reduced and differentially regulated cytolytic activity in lymphoid tissue. *Cell Rep*. 2017;21(12):3458–3470.
42. Douek DC, et al. A novel approach to the analysis of specificity, clonality, and frequency of HIV-specific T cell responses reveals a potential mechanism for control of viral escape. *J Immunol*. 2002;168(6):3099–3104.
43. Estes JD. Pathobiology of HIV/SIV-associated changes in secondary lymphoid tissues. *Immunol Rev*. 2013;254(1):65–77.
44. Musey L, et al. Ontogeny and specificities of mucosal and blood human immunodeficiency virus type 1-specific CD8$^+$ cytotoxic T lymphocytes. *J Virol*. 2003;77(1):291–300.
45. Sant S, et al. Single-cell approach to influenza-specific CD8$^+$ T cell receptor repertoires across different age groups, tissues, and following influenza virus infection. *Front Immunol*. 2018;9:1453.
46. Pizzolla A, et al. Influenza-specific lung-resident memory T cells are proliferative and polyfunctional and maintain diverse TCR profiles. *J Clin Invest*. 2018;128(2):721–733.
47. Kiniry BE, et al. Detection of HIV-1-specific gastrointestinal tissue resident CD8$^+$ T-cells in chronic infection. *Mucosal Immunol*. 2018;11(3):909–920.
48. Quigley MF, et al. Convergent recombination shapes the clonotypic landscape of the naive T-cell repertoire. *Proc Natl Acad Sci USA*. 2010;107(45):19414–19419.
49. Venturi V, et al. A mechanism for TCR sharing between T cell subsets and individuals revealed by pyrosequencing. *J Immunol*. 2011;186(7):4285–4294.
50. Brenchley JM, et al. CD4$^+$ T cell depletion during all stages of HIV disease occurs predominantly in the gastrointestinal tract. *J Exp Med*. 2004;200(6):749–759.
51. Klatt NR, et al. Compromised gastrointestinal integrity in pigtail macaques is associated with increased microbial translocation, immune activation, and IL-17 production in the absence of SIV infection. *Mucosal Immunol*. 2010;3(4):387–398.
52. Brenchley JM, et al. T-cell subsets that harbor human immunodeficiency virus (HIV) in vivo: implications for HIV pathogenesis. *J Virol*. 2004;78(3):1160–1168.
53. Klatt NR, et al. SIV infection of rhesus macaques results in dysfunctional T- and B-cell responses to neo and recall Leishmania major vaccination. *Blood*. 2011;118(22):5803–5812.
54. Mattapallil JJ, Douek DC, Hill B, Nishimura Y, Martin M, Roederer M. Massive infection and loss of memory CD4+ T cells in multiple tissues during acute SIV infection. *Nature*. 2005;434(7037):1093–1097.
55. Quigley MF, Almeida JR, Price DA, Douek DC. Unbiased molecular analysis of T cell receptor expression using template-switch anchored RT-PCR. *Curr Protoc Immunol*. 2011;Chapter 10:Unit10.33.
56. Lefranc MP, et al. IMGT, the international ImMunoGeneTics database. *Nucleic Acids Res*. 1999;27(1):209–212.